this fact, however, (2.1) and (2.16) are used extensively because they approximate the actual properties of more complex magnetic materials with sufficient accuracy over a sufficiently wide operating range.

Ferromagnetic materials, especially electrical steels, are the most common magnetic materials used in motor construction. The permeability of these materials is nonlinear and multivalued, making exact analysis extremely difficult. In addition to the permeability being a nonlinear, saturating function of the field intensity, the multivalued nature of the permeability means that the flux density through the material is not unique for a given field intensity. Rather, it is a function of the past history of the field intensity. Because of this behavior, the magnetic properties of a ferromagnetic material are often described graphically in terms of its *B-H* curve, hysteresis loop, and core losses.

Ferromagnetic Materials

Figure 2-14 shows the *B-H* curve and several hysteresis loops for a typical ferromagnetic material. Hysteresis loops are formed by applying sinusoidal excitation of different amplitudes to the material and plotting *B* versus *H*. The *B-H* curve is formed by connecting the tips or extremes of the hysteresis loops together to form a smooth curve. The *B-H* curve, or DC magnetization curve, represents an average material characteristic that reflects the nonlinear property of the permeability, but ignores its multivalued property.

Two relative permeabilities are associated with the *B-H* curve. The normalized slope of the *B-H* curve at any point is called the relative differential permeability and is given by

$$\mu_d = \frac{1}{\mu_o}\frac{dB}{dH} \tag{2.17}$$

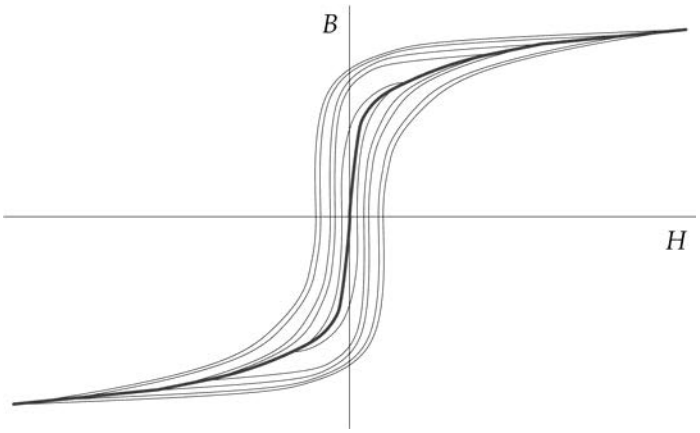

Figure 2-14. Typical ferromagnetic material magnetization characteristics.

In addition, the relative amplitude permeability is the ratio of B to H at a point on the curve,

$$\mu_a = \frac{1}{\mu_o}\frac{B}{H} \tag{2.18}$$

Both of these permeability measures are useful for describing the relative permeability of the material. Over a significant range of operating conditions, they are both much greater than one. Though not apparent from the illustrative curves shown in Fig. 2-14, the relative differential permeability is small for low field intensity, increases and peaks at medium field intensity, and finally decreases for high field intensities. At very high field intensities, μ_d approaches one and the material is said to be in hard saturation. For common electrical steels, hard saturation is reached at a flux density between 1.5 and 2.3 T and the onset of saturation occurs in the neighborhood of 1.0 to 1.5 T.

Core Loss

When ferromagnetic materials are excited with any time varying excitation, energy is dissipated due to hysteresis and eddy current losses. These losses are difficult to isolate experimentally, therefore their combined losses are usually measured and called core losses. **Figure 2-15** shows core loss density data of a typical magnetic material for sinusoidal excitation. These curves represent the loss per unit mass when the material is exposed uniformly to a sinusoidal magnetic field of various amplitudes. Total core loss in a block of material is therefore found by multiplying the mass of the material by the appropriate data value read from the graph. In brushless permanent magnet motors, different parts of the motor ferromagnetic material are exposed to different flux density amplitudes as well as waveshapes that differ significantly from sinusoidal. Therefore core loss data as shown in Fig.

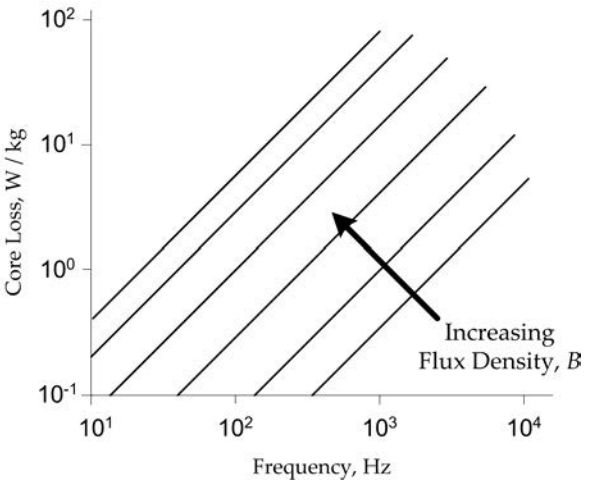

Figure 2-15. Typical core loss characteristics.

2-15 is difficult to apply to brushless permanent magnet motors. In a later chapter, techniques will be developed that permit utilization of sinusoidal core loss data for more accurate prediction of core losses in motors. Until then, it is beneficial to explore the two components of core loss.

Hysteresis loss results because energy is lost every time a hysteresis loop is traversed. This loss is directly proportional to the size of the hysteresis loop of a given material; and therefore by inspection of Fig. 2-14, it is proportional to the amplitude of the excitation. In general, hysteresis power loss is approximated by the equation

$$P_h = k_h f B_p^n$$

where k_h is a constant that depends on the material type and dimensions, f is the frequency of applied excitation, B_p is the peak flux density amplitude within the material, and n is a material dependent exponent usually between 1.5 and 2.5.

Eddy current loss is caused by electric currents induced within the ferromagnetic material under time varying magnetic excitation. These induced eddy currents circulate within the material dissipating power (*i.e.*, I^2R losses) due to the resistivity of the material. Eddy current power loss is commonly approximated by the relationship

$$P_e = k_e h^2 f^2 B_p^2$$

where h is the material thickness and k_e is a material dependent constant. Here power lost is proportional to the square of frequency, peak flux density amplitude, and material thickness in the plane perpendicular to the magnetic field flow. Therefore, one would expect hysteresis loss to dominate at low frequencies and eddy current loss to dominate at higher frequencies.

The most straightforward way to minimize eddy current loss is to increase the resistivity of the material. This is commonly done in a number of ways. First, electrical steels contain a small amount of silicon. The presence of silicon increases the resistivity of the steel substantially, thereby reducing eddy current losses. In addition, it is common to build an apparatus using laminations of material as shown in **Fig. 2-16**. These thin sheets of material are coated with a thin layer of insulating material. Stacking these insulated laminations together dramatically increases the resistivity of the material in the direction of the stack. Since the insulating material is also nonmagnetic, it is necessary to orient the lamination edges parallel to the desired flow of flux. As described by the equation above, eddy current loss is proportional to the square of the lamination thickness. Thus, thin laminations are required for lower loss operation at high frequencies.

Laminations decrease the amount of magnetic material available to carry flux within a given cross-sectional area. To compensate for this decrease, a stacking

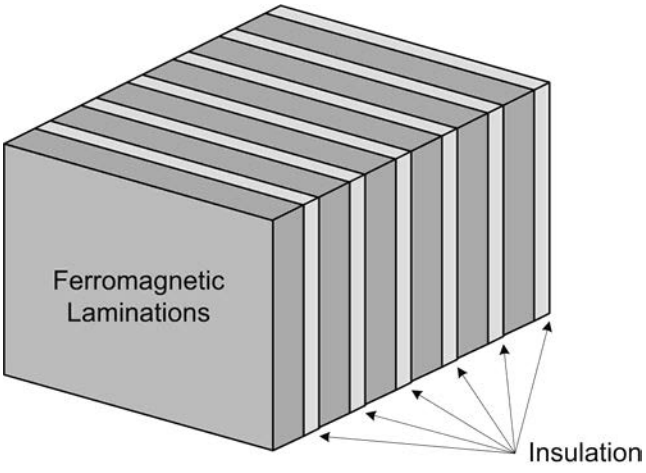

Figure 2-16. Laminated ferromagnetic material.

factor is defined as the ratio of the steel cross-sectional area to the total cross-sectional area occupied by the stacked laminations, *i.e.*,

$$K_{st} = \frac{A_{st}}{A_{total}} \tag{2.19}$$

This factor expresses the normalized amount of the total cross-sectional area and is important for the accurate calculation of flux densities in laminated magnetic materials. Typical stacking factors range from 0.8 to 0.99.

Though not used extensively in motor construction, powdered ferromagnetic materials can be used to reduce eddy current loss and allow for three dimensional flux flow. These materials may become very popular. They are composed of powdered magnetic material suspended in a nonconductive resin. The small particle size and their electrical isolation from one another dramatically increase the effective resistivity of the material. However, in this case the effective permeability of the material is decreased because the nonmagnetic resin appears in all flux paths through the material.

Permanent Magnets

Many different types of permanent magnet materials are available today. The types available include alnico, ferrite (ceramic), samarium-cobalt (SmCo), and neodymium-iron-boron (NdFeB). Of these, ferrite types are the most popular because they are inexpensive. On the other hand, the rare earth types, SmCo and NdFeB offer the highest performance. NdFeB magnets are more popular in higher performance applications because they are much less expensive than SmCo. Most magnet types are available in both bonded and sintered forms. Bonded magnets are formed by suspending powdered magnet material in a nonconductive, non-

magnetic resin. Magnets formed in this way are not capable of high performance since a substantial fraction of their volume is made up of nonmagnetic material. The magnetic material used to hold trinkets to your refrigerator door is bonded, as is the magnetic material in the refrigerator door seal. Sintered magnets, on the other hand, are capable of high performance because the sintering process allows magnets to be formed without a bonding agent. Overall, each magnet type has different properties leading to different constraints and different levels of performance in brushless permanent magnet motors. Rather than exhaustively discussing each of these magnet types, this text discusses only generic properties.

Stated in the simplest possible terms, permanent magnets are magnetic materials with large hysteresis loops. Thus, the starting point for understanding permanent magnet is their hysteresis loop, the first and second quadrant of which are shown in **Fig. 2-17**. For convenience, the field intensity axis is scaled by μ_o, giving both axes dimensions in Tesla. (Note: This scaling also visually compresses the field intensity axis. The uncompressed slope of the line in the second quadrant is approximately μ_o, which is very small.) The hysteresis loop shown in the figure is formed by applying the largest possible field intensity to an unmagnetized sample of material, then shutting it off. This shutting off allows the material to relax, or recoil, along the upper curve shown in the figure, which is called the demagnetization curve. The final position attained is a function of the magnetic environment in which the magnet is placed.

If the two ends of the magnet are shorted together by a piece of infinitely permeable material (an infinite permeance) as shown in **Fig. 2-18***a*, the magnet is said to be keepered, and the final point attained is $H = 0$. The flux density leaving the magnet at this $H = 0$ point is equal to the remanence, or residual induction, denoted B_r. The remanence is the maximum flux density that the magnet can produce by itself. On the other hand, if the permeability surrounding the magnet is zero (a permeance of zero) as shown in Fig. 2-18*b*, no flux flows out of the magnet, and the final point attained is $B = 0$. At this $B = 0$ point, the magnitude of the field intensity across the magnet is equal to the negative of the coercivity or coercive

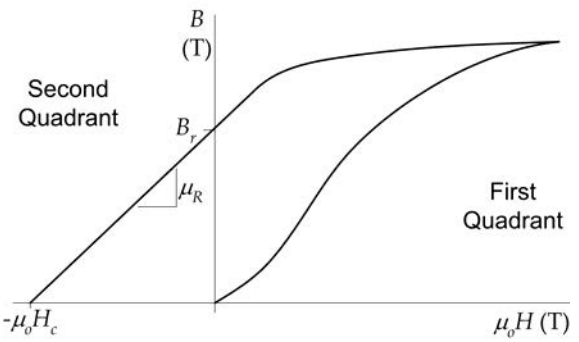

Figure 2-17. The *B-H* loop of a permanent magnet.

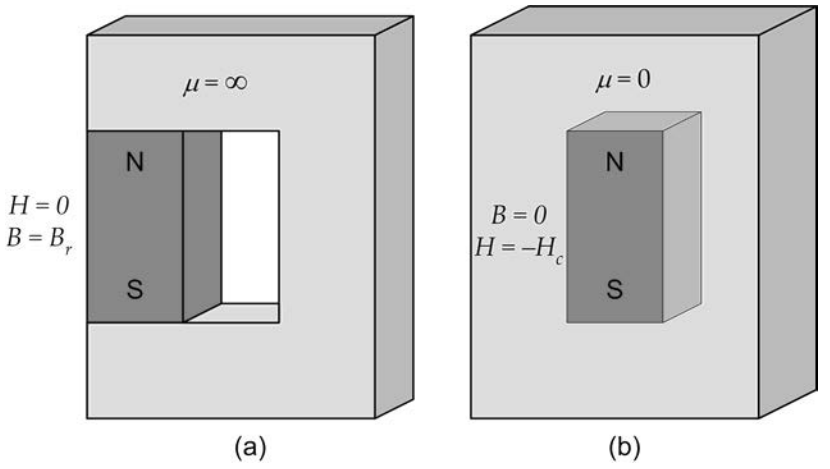

Figure 2-18. Operation of a permanent magnet at its (a) remanence, and (b) coercivity.

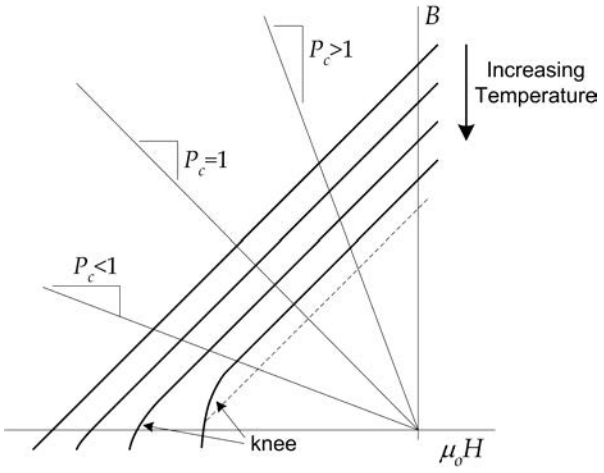

Figure 2-19. Influence of temperature on the demagnetization curve.

force, denoted H_c, because H_c is stated as a positive value on permanent magnet specifications. For permeance values between zero and infinity, the operating point lies somewhere in the second quadrant, *i.e.*, between the remanence and coercivity. The magnitude of the slope of a line drawn from a point on the curve to the origin is known as the permeance coefficient, denoted P_c. Therefore, in terms of P_c, a permeance coefficient equal to zero is operation at the coercivity $B = 0$, $H = -H_c$, and a permeance coefficient equal to infinity is operation at the remanence $B = B_r$, $H = 0$.

Permanent magnet materials such as SmCo and NdFeB materials have straight demagnetization curves throughout the second quadrant at room temperature as shown in **Fig. 2-19**. Some ferrite magnets have a knee or bend in their demagnetiz-

ation curve at room temperature and at low flux density values. The slope of the straight line demagnetization curve in the second quadrant is equal to μ_R, where μ_R is the relative recoil permeability of the material. For ceramic, SmCo, and NdFeB magnets, the value of μ_R is typically between 1.0 and 1.2. At higher temperatures, the demagnetization curve shrinks toward the origin as shown in Fig. 2-19. As the demagnetization curve shrinks toward the origin, the flux available from the magnet drops, reducing the performance of the magnet. However, this performance degradation is reversible as the demagnetization curve returns to its former shape as temperature decreases. The effect of temperature on the remanence B_r is approximately linear, and can therefore be described by

$$B_r(T) = B_r(T_o)\left[1 + \Delta_B(T - T_o)\right] \tag{2.20}$$

where T is the magnet temperature, T_o is a reference temperature, $B_r(T_o)$ is the remanence at T_o, and Δ_B is the reversible temperature coefficient.

In addition to shrinking toward the origin as temperature increases, a knee in the demagnetization characteristic of SmCo and NdFeB materials may move into the second quadrant as shown in Fig. 2-19. This deviation from a straight line causes the flux density to drop off more quickly as $-H_c$ is approached. Operation in the area of the knee can cause the magnet to lose some magnetization irreversibly because the magnet will recoil along a line of lower magnetization as shown by the dashed line in Fig. 2-19. If this change in recoil line occurs, the effective B_r and H_c drop, lowering the performance of the magnet. Since this change is undesirable, it is necessary to ensure that magnets operate away from the coercivity at a sufficiently large permeance coefficient P_c.

The demagnetization curve shown in Figs. 2-17 and 2-19 is known as the normal demagnetization curve. This curve describes how a magnet behaves in a magnetic circuit and therefore is useful in motor design. In addition to this curve, magnets are also described in terms of an intrinsic demagnetization curve. This intrinsic curve describes the inherent magnetization characteristics of the magnet independent of its environment. This intrinsic curve is intimately related to the normal demagnetization curve, but is generally not directly useful for motor design.

Finally, before moving on, it is beneficial to define the maximum energy product, as this specification is usually the first specification used to compare magnets. The maximum energy product BH_{max} of a magnet is the maximum product of the flux density and field intensity along the magnet demagnetization curve. Even though this product has units of energy, it is not actual stored magnet energy, but rather it is a qualitative measure of a magnet's performance capability in a magnetic circuit. By convention, BH_{max} is usually specified in the English units of millions of Gauss-Oersteds (MG·Oe). However, some magnet manufacturers do conform to SI units units of Joules per cubic meter (1MG·Oe = 7.958 kJ/m^3). For magnets with $\mu_R \approx 1$, BH_{max} occurs near the unity permeance coefficient operating point. It can be shown that operation at BH_{max} is the most efficient in terms of magnet volumetric energy

density. That is, operation at BH_{max} provides the greatest usable magnet energy for the least magnet material. Despite this fact, permanent magnets in motors are almost never operated at BH_{max} because of possible irreversible demagnetization with increasing temperature as discussed in the previous paragraph.

Permanent Magnet Magnetic Circuit Model

To move the magnet operating point from its static operating point determined by the external permeance, an external magnetic field must be applied. In a motor, the static operating point lies somewhere in the second quadrant, usually at a permeance coefficient of three or more. When motor windings are energized, the operating point dynamically varies following minor hysteresis loops about the static operating point as shown in **Fig. 2-20**. These loops are thin and have a slope essentially equal to that of the demagnetization characteristic. As a result, the trajectory closely follows the overall straight line demagnetization characteristic described by

$$B_m = B_r + \mu_R \mu_o H_m \tag{2.21}$$

where H_m is a negative quantity because operation is in the second quadrant. This equation assumes that the magnet remains in a linear operating region under all operating conditions. Driving the magnet past the remanence into the first quadrant normally causes no harm, as this is in the direction of magnetization. However, if the external magnetic field opposes that developed by the magnet and drives the operating point into the third quadrant past the coercivity, it is possible to irreversibly demagnetize the magnet if operation drives the magnet into a knee region.

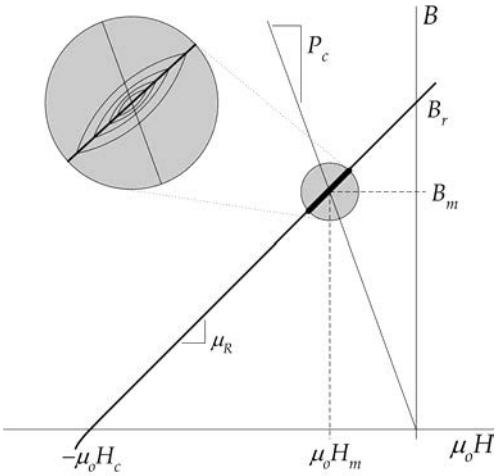

Figure 2-20. Dynamic operation of a permanent magnet around an operating point.

Using (2.21), it is possible to develop a magnetic circuit model for a permanent magnet. Let the rectangular magnet shown in **Fig. 2-21**, be described by (2.21). Then the flux leaving the magnet is

$$\phi = B_m A_m = B_r A_m + \mu_R \mu_o A_m H_m$$

where A_m is the cross-sectional area of the magnet face through which the flux flows. Using (2.4), (2.5), and (2.6), this equation can be rewritten as

$$\phi = \phi_r + P_m F_m \tag{2.22}$$

where

$$\phi_r = B_r A_m \tag{2.23}$$

is a fixed flux source, and where

$$P_m = \frac{\mu_r \mu_o A_m}{l_m} \tag{2.24}$$

is the permeance of the magnet. Conventionally (2.24) is called the magnet leakage permeance, although here it will simply be called the magnet permeance. Equation (2.22) implies that the magnetic circuit model for the magnet is a flux source in parallel with a permeance as shown in Fig. 2-21, *i.e.*, summing the fluxes ϕ_r and $P_m F_m$ gives the net flux ϕ. It is important to recognize that this model assumes that the physical magnet is uniformly magnetized over its cross section and is magnetized in its preferred direction of magnetization.

When the magnet shape differs from the rectangular shape shown in Fig. 2-21, it is necessary to reevaluate its magnetic circuit model. In brushless permanent magnet motors that have a radial air gap, the magnet shape may appear as an arc as shown in **Fig. 2-22**. The magnetic circuit model of this shape can be found by considering it to be a radial stack of differential length magnets, each having a model as given in Fig. 2-21. During magnetization the same amount of flux magnetizes

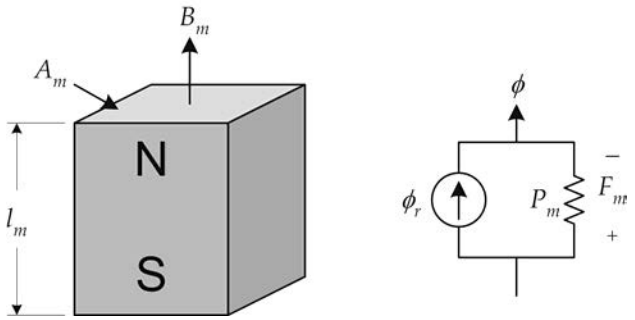

Figure 2-21. A rectangular permanent magnet and its magnetic circuit model.

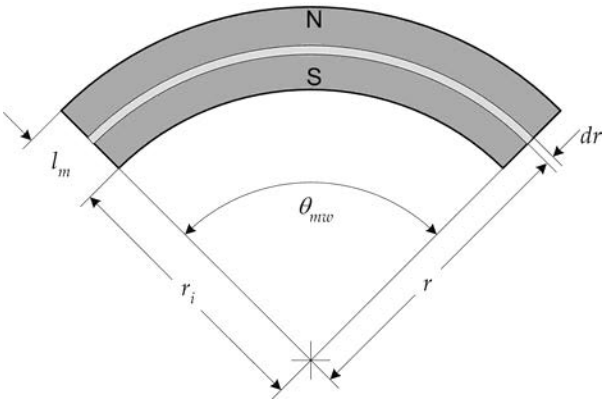

Figure 2-22. An arc-shaped permanent magnet magnetized radially.

each differential length. As a result, the achieved remanence decreases linearly with increasing radius because the same flux over a increasing area gives a smaller flux density.

To derive the magnetic circuit model for the arc-shaped magnet in Fig. 2-22, consider a differential slice of radial thickness *dr* as shown in the figure. This slice has a differential reluctance of

$$dR = \frac{dl}{\mu A} = \frac{dr}{\mu r \theta_{mw} L}$$

where *L* is the depth of the magnet into the page. Because reluctances add in series just as resistors do, the net reluctance of the magnet is given by the sum, *i.e.*, integral, of each differential reluctance

$$R_m = \int_{r_i}^{r_i+l_m} dR = \int_{r_i}^{r_i+l_m} \frac{1}{\mu_R \mu_o L \theta_{mw} r} dr = \frac{\ln\left(1+l_m/r_i\right)}{\mu_R \mu_o L \theta_{mw}} \tag{2.25}$$

The inverse of this reluctance is the magnet permeance P_m as shown in Fig. 2-21

$$P_m = \frac{\mu_R \mu_o L \theta_{mw}}{\ln\left(1+l_m/r_i\right)} \tag{2.26}$$

Using the fact that the same flux flows through each slice during the magnetization process, the flux source is given by the remanence acting over the surface at r_i

$$\phi_r = B_r A = B_r L \theta_{mw} r_i \tag{2.27}$$

It is interesting to note that in the common case where $l_m \ll r_i$, the magnet permeance expression (2.26) simplifies to

$$P_m = \frac{\mu_R \mu_o L \theta_{mw} r_i}{l_m} \tag{2.28}$$

which is equivalent to the permeance of a rectangular block having width $w_m = \theta_{mw} r_i$ and length l_m. That is, the magnet appears to have a constant width given by the arc width at r_i, not at the average radii $r_i + l_m/2$.

2.3 Example

To illustrate the concepts presented in this chapter, consider the magnetic apparatus and circuit shown in **Fig. 2-23**. The apparatus consists of a permanent magnet, highly permeable ferromagnetic material, and an air gap. Given that the ferromagnetic material has very high permeability, its reluctance can be ignored, resulting in a magnetic circuit consisting of the magnet equivalent circuit and the air gap permeance as shown in the figure.

Since the flux leaving the magnet is equal to the flux crossing the air gap, *i.e.*, $B_m A_m = B_g A_g$, the magnet and air gap flux densities are related by

$$B_g = B_m \frac{A_m}{A_g} = B_m C_\phi \tag{2.29}$$

where A_m and A_g are the cross-sectional areas of the magnet and air gap respectively and

$$C_\phi = \frac{A_m}{A_g} \tag{2.30}$$

is the flux concentration factor. When C_ϕ is greater than one, the flux density in the air gap is greater than that at the magnet surface. Likewise, when C_ϕ is less than one, the flux density in the air gap is less than that at the magnet surface

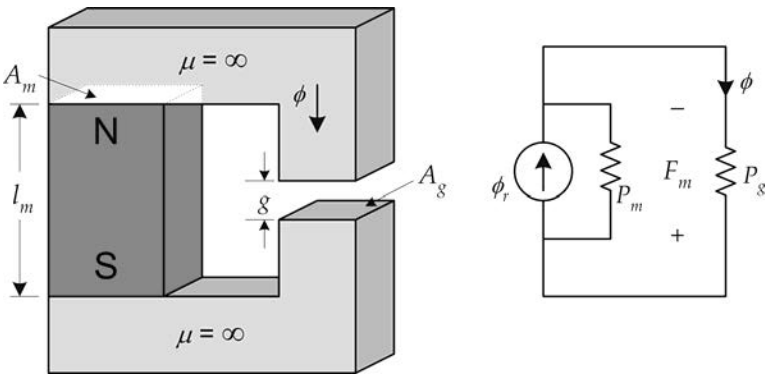

Figure 2-23. A simple magnetic structure and its magnetic circuit model.

The flux ϕ is easily found by flux division (*i.e.*, just as one uses current division in an electric circuit),

$$\phi = \phi_r \frac{P_g}{P_g + P_m}$$

If the air gap is modeled simply as $P_g = \mu_o A_g / g$, then this equation can be rewritten as

$$\phi = \frac{\phi_r}{1 + \left(\frac{\mu_R g}{l_m} \right) C_\phi} \tag{2.31}$$

Knowing ϕ, the MMF across the circuit as defined in the figure is

$$F_m = \frac{-\phi_r}{P_m + P_g} = \frac{-B_r A_m}{\mu_R \mu_o \left(\frac{A_m}{l_m} + \frac{A_g}{\mu_R g} \right)} \tag{2.32}$$

These two equations describe the flux and MMF solutions of the magnetic circuit. As stated, the two equations do not provide any significant insight into the operation of the circuit. There are simply too many variables in the equations. However, recognizing that $B_m = \phi / A_m$ and $H_m = F_m / l_m$, the permeance coefficient defining the operating point is given by

$$P_c = \frac{-B_m}{\mu_o H_m} = \frac{l_m}{g} \frac{1}{C_\phi} \tag{2.33}$$

This remarkably simple result says that the ratio of the magnet length to the air gap length and the flux concentration factor determine the permeance coefficient. Since the permeance coefficient must be greater than one for safe operation of the magnet especially at higher temperatures, the magnet length must be significantly larger than the air gap length. Moreover, any attempt to increase the air gap flux density through flux concentration, *i.e.*, $C_\phi > 1$, pushes the permeance coefficient lower.

The fundamental importance of (2.33) can be seen by considering what is required to maintain a constant permeance coefficient as the flux concentration factor increases. Multiplying the numerator and denominator of (2.33) by $A_m A_g$ and simplifying gives

$$P_c = \frac{V_m}{V_g} \frac{1}{C_\phi^2} \tag{2.34}$$

where V_m and V_g are the magnet and air gap volumes respectively. If C_ϕ is doubled to $2C_\phi$ and the air gap volume remains constant, the magnet volume must increase by a factor of $2^2 = 4$ to maintain a constant permeance coefficient. If the magnet cross-sectional area remains constant, this implies that the magnet length must increase by a factor of 4. The implication of this analysis is that concentrating the flux of a permanent magnet comes with the penalty of geometrically increasing magnet volume.

2.4 Summary

In this chapter, the basics of magnetic circuit analysis were presented. Starting with fundamental magnetic field concepts, the concepts of permeance, reluctance, flux, and MMF were developed. Permeance models for blocks of magnetic material, air gaps and slotted magnetic structures were developed. The properties of ferromagnetic and permanent magnet materials were discussed. A magnetic circuit model of a permanent magnet was introduced and the concept of flux concentration was illustrated.

With this background it is now possible to discuss how magnetic fields interact with the electrical and mechanical parts of a motor. These concepts are discussed in the next chapter.

3 Electrical and Mechanical Relationships

As stated in the first chapter, the operation of a brushless permanent magnet motor relies on the conversion of electrical energy to magnetic energy and from magnetic energy to mechanical energy. In this chapter, the connections between magnetic field concepts, electrical circuits, and mechanical motion will be explored to illustrate this energy conversion process.

3.1 Flux Linkage and Inductance

Self Inductance

To define flux linkage and self inductance, consider the magnetic circuit shown in **Fig. 3-1**. This circuit is said to be singly excited since it has only one coil to produce a magnetic field. The flux ϕ flowing around the core is due to the current i and the direction of flux flow is clockwise because of the right hand rule. Using the magnetic circuit equivalent of Ohm's law, the flux produced is given by

$$\phi = \frac{Ni}{R} \tag{3.1}$$

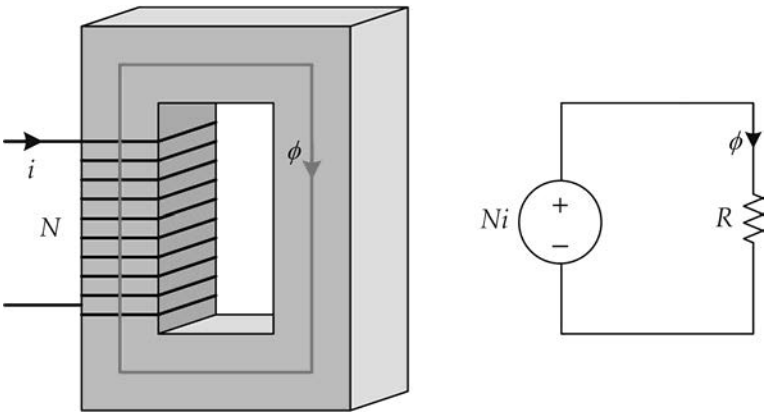

Figure 3-1. Single excited magnetic structure and its magnetic circuit model.